



# Control of Chaos by Nonfeedback Methods in a Simple Electronic Circuit System and the FitzHugh–Nagumo Equation

S. RAJASEKAR

<sup>a</sup>Department of Physics, Manonmaniam Sundaranar University, Tirunelveli 627 002, India

K. MURALI and M. LAKSHMANAN

Centre for Nonlinear Dynamics, Department of Physics, Bharathidasan University, Tiruchirappalli 620 024, India

**Abstract**—Various control algorithms have been proposed in recent years to control chaotic systems. These methods are broadly classified into feedback and nonfeedback methods. In this paper, we make a critical analysis of nonfeedback methods such as (i) addition of constant bias, (ii) addition of second periodic force, (iii) addition of weak periodic pulse, and (iv) entrainment control. We apply these methods to a simple electronic circuit, namely, the Murali–Lakshmanan–Chua circuit system and FitzHugh–Nagumo equation. We make a comparative study of the various features associated with the algorithms. © 1997 Elsevier Science Ltd

## 1. INTRODUCTION

Chaotic systems are well-known for their extreme sensitivity to small uncertainties in their initial conditions and this inherent nonlinear phenomenon is often undesirable in many practical considerations. Thus one may wish to avoid or control chaotic motion in such situations. In recent years, a great deal of interest has been paid to develop effective control algorithms [1–18]. The existing control algorithms can be classified, mainly, into two categories: feedback and nonfeedback. Feedback methods [1–7] are primarily devised to control chaos by stabilizing a desired unstable periodic orbit embedded in a chaotic attractor. In practice, one first tracks the desired orbit and then applies the necessary changes in the system parameter. The required perturbation is proportional to the deviation of the actual trajectory to the desired trajectory. The perturbation is generally nonperiodic and is to be calculated every instant.

The nonfeedback methods [8–16] suppress chaotic motion by converting the system dynamics to a periodic orbit. In these methods, one does not perform changes in the system according to its position in phase space, but applies instead weak periodic perturbations on some control parameters or variables. The essential advantages of nonfeedback technique lies in their speed, flexibility and no online monitoring and processing requirements. The flexibility and speed make them especially promising for controlling systems such as chaotic circuits, fast electro-optical systems, and so on. The nonfeedback methods include weak periodic parametric perturbation [8] addition of second periodic force [9], constant bias [15, 16], addition of weak periodic pulses, open-loop entrainment control [11] and addition of weak noise signal [12, 14].

The goal of this paper is to apply the nonfeedback methods to the simplest nonlinear

Table 1. This table gives the form of the various nonfeedback controls considered in the present analysis. The general form of the controlled dynamical system is  $\dot{x} = F(x) + C(t)$ , where  $C(t)$  is the perturbation introduced to control chaos

Number	Method	Controller	Special features
1	Constant bias	$C(t) = C_0 = \text{constant}$	Perturbation is constant and is easy to implement in dynamical systems. Before implementation system dynamics must be known for various values for $C_0$ .
2	Addition of weak periodic force	$C(t) = \eta \sin \Omega t$	Easy to implement in mechanical and electrical circuit systems. Suppression of chaos occurs only for certain range of values of $\eta$ and $\Omega$ .
3	Weak periodic pulses	$C(t) = \alpha \sum_{n=1}^{\infty} \delta(t - n\tau)$	Perturbation is added to the system only at discrete times. System dynamics must be studied in $(\alpha, \tau)$ space in order to choose suitable values of $\alpha$ and $\tau$ to eliminate chaos.
4	Entrainment control	$C(t) = (\dot{g} - F(g))\mathcal{S}(t)$	Any arbitrary goal dynamics $g$ can be stabilized. Evolution equation of the chaotic system is required and a particular solution of the system cannot be entrained. $\mathcal{S}(t)$ is a switching function.

dissipative non-autonomous circuit, namely, the circuit introduced recently by Murali, Lakshmanan and Chua [16, 17] and to the FitzHugh–Nagumo (FN) equation. In Table 1, we summarize the form of the controllers, their most important characteristic properties and their notable advantages and disadvantages.

In Section 2, we consider the influence of the addition of constant bias and second periodic force on the chaotic dynamics. We show suppression of chaos for a range of values of constant bias and amplitude of the second periodic force in both the Murali–Lakshmanan–Chua (MLC) circuit as well as in its dynamical equation. Section 3 is devoted to the study of suppression of chaos in the MLC circuit equation by weak periodic delta function force. Regular behaviour is found to occur for a wide range of amplitude and frequency of the applied force. Suppression of chaos is also observed when a weak periodic rectangular force is applied to the system. In Section 4, we illustrate the entrainment control now in the FN system. For a periodically driven MLC system, the equation of motion of the entrainment controlled system does not contain periodic force. This is equivalent to the study of the system free from the external periodic force. In such a system, chaotic motion does not exist. So we choose an autonomous system, namely the FitzHugh–Nagumo equation to study the entrainment control. We illustrate the entrainment of FN system dynamics to a chosen stationary point solution and to a periodic orbit. Finally, Section 5 contains a summary and conclusions.

## 2. CONTROLLING OF CHAOS IN MLC CIRCUIT BY WEAK CONSTANT BIAS AND WEAK PERIODIC SIGNAL

### 2.1. Effect of constant bias

The circuit realization of the simplest dissipative chaotic nonlinear circuit, namely, the MLC circuit, is shown in Fig. 1. It contains a linear capacitor ( $C$ ), a linear inductor ( $L$ ), a linear

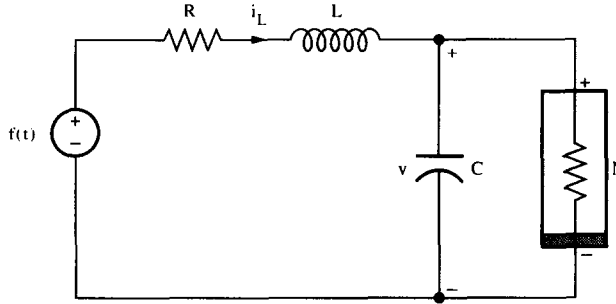


Fig. 1. Circuit diagram of the MLC circuit;  $R = 1360 \Omega$ ,  $L = 18 \text{ mH}$ ,  $C = 10 \text{ nF}$  and the frequency of the external force is 8890 Hz.

resistor ( $R$ ) and a nonlinear element ( $N$ ) which is the Chua's diode and an external periodic forcing source. The time variation of voltage  $v$  across the capacitor  $C$  and the current  $i_L$  through the inductor  $L$  are represented by the set of differential equations

$$C \frac{dv}{dt} = i_L - g(v), \quad (1a)$$

$$L \frac{di_L}{dt} = -Ri_L - v + f \sin(\Omega t), \quad (1b)$$

where  $f$  is the amplitude,  $\Omega$  is the frequency of the external periodic signal and  $g(v)$  represents the  $v$ - $i$  characteristic of the Chua's diode and is given [16] by

$$i_N = g(v) = G_b v + 0.5(G_a - G_b)(|v + B_p| - |v - B_p|). \quad (1c)$$

By suitably rescaling the variables and parameters, these equations can be written in dimensionless form as [16]

$$\dot{x} = y - g(x), \quad (2a)$$

$$\dot{y} = -\sigma y - \beta x + F \sin(\omega t), \quad (2b)$$

where

$$g(x) = bx + 0.5(a - b)[|x + 1| - |x - 1|]. \quad (2c)$$

In these equations,  $\sigma$ ,  $\beta$ ,  $a$  and  $b$  are rescaled circuit parameters of equations (1a)–(1c).

A variety of dynamical behaviours including chaotic motion have been observed in the circuit system (1) experimentally and verified numerically in equations (2a)–(2c). For example, chaotic behaviour is found in the circuit for the specific choice [16] of the parameters  $C = 10 \text{ nf}$ ,  $L = 18 \text{ mH}$ ,  $R = 1360 \text{ ohm}$ ,  $G_a = -0.76 \text{ ms}$ ,  $G_b = -0.41 \text{ ms}$ ,  $B_p = 1.0 \text{ V}$ , frequency of the external periodic force  $\Omega/2\pi = 8890 \text{ Hz}$  and  $f = 0.107 V_{\text{rms}}$ , as shown in Fig. 2(a). For these experimental circuit parametric choices, the values of  $\beta$ ,  $\sigma$ ,  $\omega$  and  $F$  in equations (2a)–(2c) are calculated [16] as 1.0, 1.015, 0.75 and 0.15, respectively. When equations (2a)–(2c) are numerically integrated for these parametric values, a double scroll type chaotic attractor is found to occur as shown in Fig. 2(b). We now study the suppression

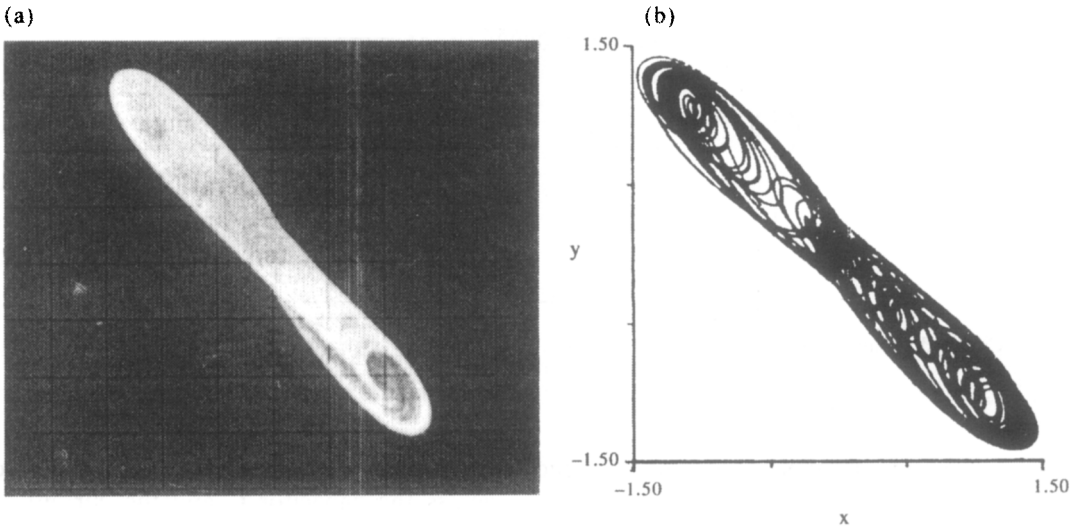


Fig. 2. (a) Chaotic attractor of Fig. 1 in  $V-u_L$  plane for  $t = 0.107 V_{lim}$ , (b) Chaotic attractor of (2) for  $\sigma = 1.015$ ,  $\beta = 1$ ,  $F = 0.15$ ,  $\omega = 0.75$ ,  $a = -1.02$ ,  $b = -0.55$ .

of chaos in the circuit system (1) and or its equivalent dynamical equations (2a)–(2c) by the addition of constant bias.

In order to suppress chaos in the MLC circuit system, it is augmented by a constant bias voltage source  $E$  in series with the periodic signal  $f(t)$ , as shown in Fig. 3. The presence of the bias element leads to the addition of a constant parameter (bias term)  $E' = \beta E/B_p$  to the right-hand side of equation (2b). Suppression of chaos is studied by varying the constant bias in the circuit as well as in its dynamical equations (2a)–(2c). The nature of the controlled orbit is same in the circuit as well as in equations (2a)–(2c). Suppression of chaos is found for a range of values of the constant bias. For example, a period- $2T$  attractor (where  $T = 1/8890$  Hz) is found for  $E = 0.03$  V while a period- $T$  orbit is found for  $E = 0.05$  V. These controlled orbits are shown in Fig. 4. To understand the route to suppression of chaos, the bifurcation phenomenon is studied for equations (2a)–(2c). Figure 5(a) shows the one-parameter bifurcation diagram in the  $(x-E')$  plane. The corresponding maximal Lyapunov exponent spectrum is plotted in Fig. 5(b). Suppression of chaos is by reverse period doubling. A similar route to suppression of chaos has also been found in the FitzHugh–Nagumo equation [15] earlier.

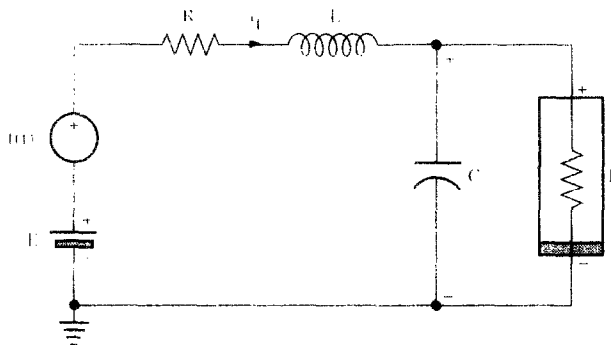


Fig. 3. MLC circuit with a constant bias voltage  $E$ .

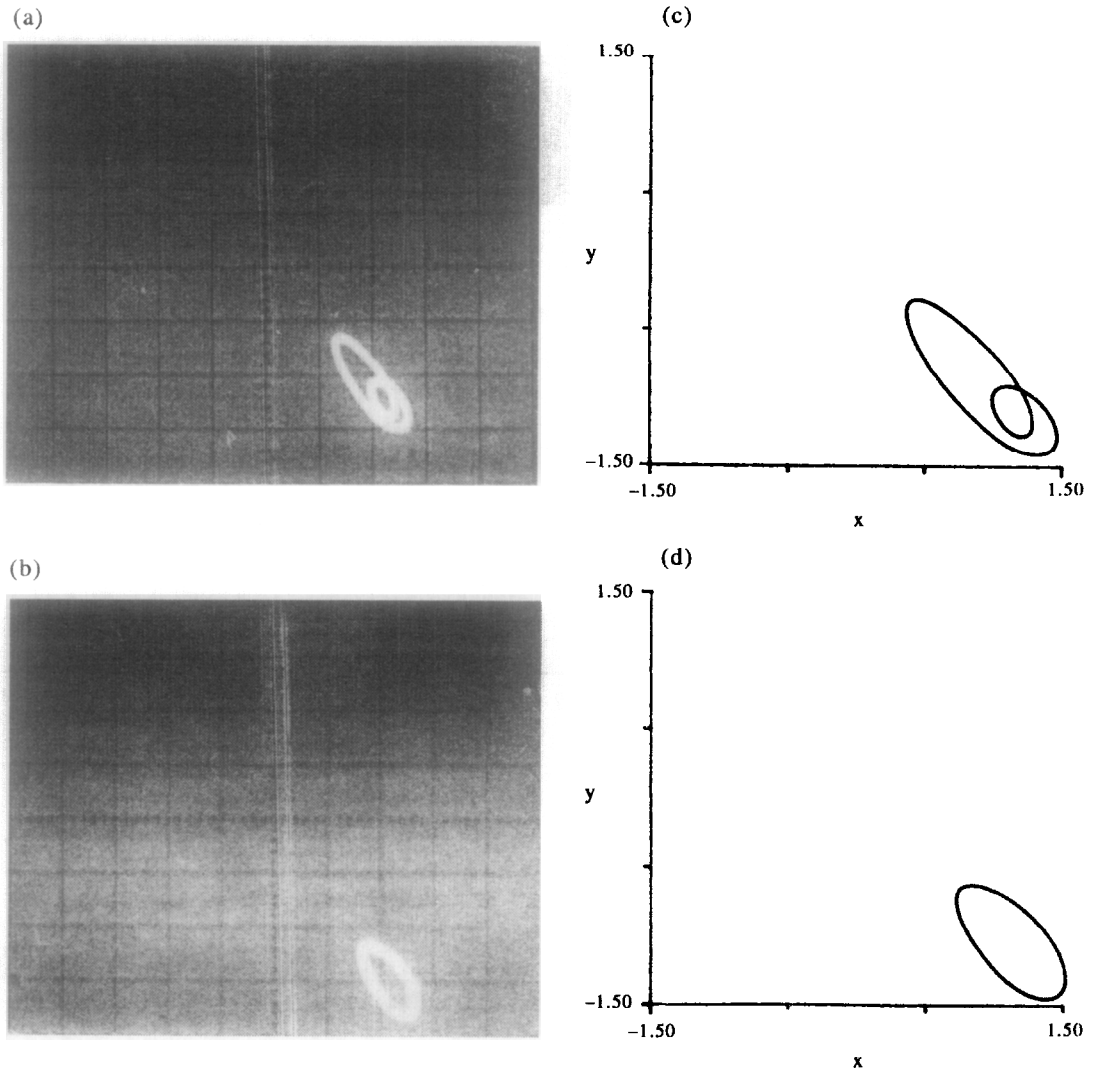


Fig. 4. (a) and (b) Periodic attractors of the MLC circuit with the constant bias: (a)  $E = 0.03$  V, (b)  $0.05$  V. (c) and (d) Periodic orbits of eqns (2) with the addition of constant bias term  $E' = \beta E/B_p$ : (c)  $E' = 0.03$ , (d)  $E' = 0.05$ .

## 2.2. Effect of second weak periodic force

One can also control chaotic dynamics by the addition of a weak second periodic force. We add a second periodic signal in series with the existing one of the MLC circuit (Fig. 1). The total forcing signal now becomes  $f_1 \sin(\Omega_1 t) + f_2 \sin(\Omega_2 t)$  and the system becomes a quasiperiodically driven one. The corresponding dynamical equation in dimensionless form is given by

$$\dot{x} = y - g(x), \quad (3a)$$

$$\dot{y} = -\sigma y - \beta x + F_1 \sin(\omega_1 t) + F_2 \sin(\omega_2 t), \quad (3b)$$

where  $F_1 = 0.15$  and  $\omega_1 = 0.75$ . Investigation has been carried out for the circuit for a fixed value of the frequency of the second force and varying the amplitude  $F_2$  over a range. We fix  $\Omega_2/2\pi = 8890$  Hz which corresponds  $\omega_2 = 0.75$ . Equations (3a) and (3b) are studied for

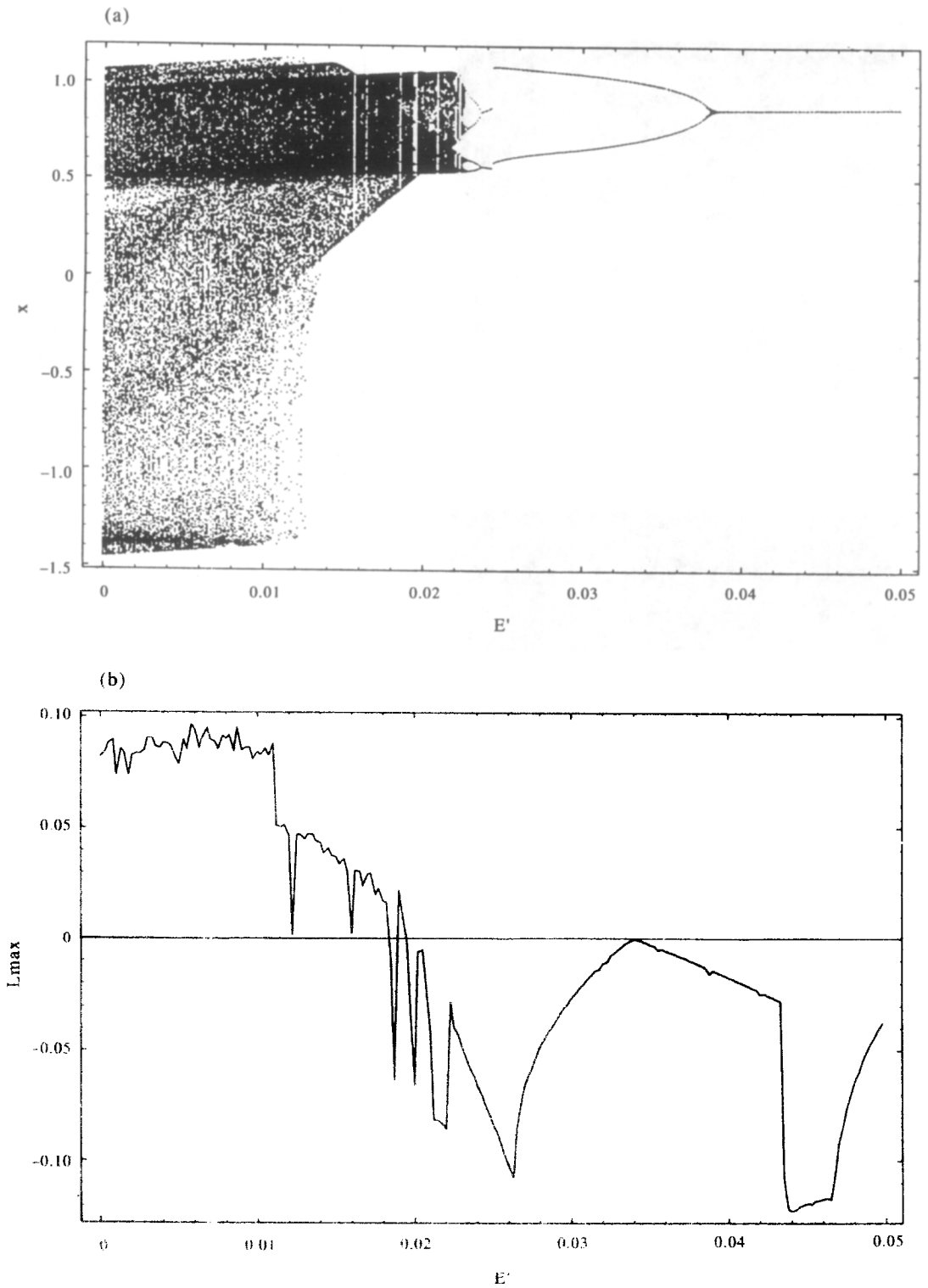


Fig. 5 (a) Bifurcation diagram and (b) corresponding maximal Lyapunov exponent of eqns (2) in the presence of constant bias  $E'$ .

$0 < F_2 < 0.2$ . Regular motion is recovered for a range of values of amplitude of the second force. Chaotic motion persists for  $0 \leq F_2 \leq 0.032$ . Suppression of chaos is observed for  $0.032 \leq F_2 \leq 0.2$ . Figure 6 shows the bifurcation phenomenon as a function of  $F_2$ . In the chaos controlled region period- $3T$  orbit is found to occur. Figure 7 shows the controlled period- $3T$  orbit in the MLC circuit and in equations (3a) and (3b).

A prime advantage of addition of periodic sinusoidal force is its easy implementability experimentally. A disadvantage is that, in general, one has to identify regular and chaotic regions in the  $(F_2, \omega_2)$  parameters space to choose suitable values of  $F_2$  and  $\omega_2$  to realize periodic motion.

### 3. CONTROLLING OF CHAOS BY WEAK PERIODIC DELTA-PULSES

In the previous two sections, we have studied the controlling of chaos by constant bias and addition of second periodic force. In these approaches, the external perturbation is continuous. It is important to investigate the controlling of chaos by adding perturbations or disturbances at discrete times only. In this section, we show that chaos can be suppressed by instantaneous burst or a weak periodic  $\delta$ -pulses and rectangular pulses. We illustrate this with reference to the MLC circuit equation.

The MLC circuit equation with a periodic  $\delta$ -pulses is given by

$$\dot{x} = y - g(x), \quad (4a)$$

$$\dot{y} = -\sigma y - \beta x + F \sin(\omega t) + \alpha \sum_{n=1}^{\infty} \delta(t - n\tau T). \quad (4b)$$

The added force is nonzero only at times  $t = n\tau T$ ,  $n = 1, 2, \dots$ . For simplicity,  $T$  is fixed as  $2\pi/\omega$ . The effect of the force is to shift  $(x, y)$  to  $(x, y + \alpha)$  at  $t = n\tau T$ . For fixed value of  $T$ , the times at which the  $\delta$ -function force becomes nonzero and the period of the force are characterized by  $\tau$ . In the absence of the  $\delta$ -force, chaotic motion is observed in equations (4a) and (4b) for  $\sigma = 1.015$ ,  $\beta = 1$ ,  $a = -1.02$ ,  $b = -0.55$ ,  $\omega = 0.75$  and  $F = 0.1$ . Equations (4a) and (4b) are integrated using the fourth-order Runge–Kutta method with time step  $2\pi/100\omega$ . The first 1000 drive cycles are discarded as transient. Figure 8 shows the bifurcation diagram as a function of  $\alpha$ , where the value of  $\tau$  is fixed at 0.5. That is, the  $\delta$ -force is nonzero and its amplitude become  $\alpha$  twice during one period of the external force  $F \sin \omega t$  at  $T/2$  and  $T$ . Chaotic behaviour persists for  $\alpha \leq 0.0145$ . An interesting point here is the suppression of chaos by inverse period-doubling phenomenon. Period  $8T$ ,  $4T$ ,  $2T$  motions are found in the intervals 0.015–0.016, 0.0165–0.0175 and 0.0180–0.0675, respectively. For  $\alpha \geq 0.068$ , period- $T$  attractor is found. For  $\tau = 0.25$ , regular motion is found for  $\alpha \geq 0.067$ . Next,  $\alpha$  is kept at 0.02 and the period of the applied force is varied. The value of  $\tau$  is increased from small value in steps of 0.01 up to 1. Regular behaviour is observed for  $0.01 \leq \tau \leq 0.054$ . The above observation indicates that one can effectively suppress chaos by applying periodic weak  $\delta$ -force with properly chosen amplitude and period.

In numerical simulation, an instantaneous burst can be easily implemented. However, in a real experimental system this is difficult. What happens if the  $\delta$ -force is nonzero within a small interval  $n\tau T \pm t'$ , where  $t'$  is small? This practical problem has also been investigated. Instead of choosing  $\delta(t)$  nonzero exactly at  $t = n\tau T$ , it is chosen nonzero at one of the times  $n\tau T$ ,  $n\tau T \pm \Delta t$ , randomly for each value of  $n$ . Here  $\Delta t$  is the time step used in the numerical integration algorithm. Figure 9 shows the bifurcation diagram for  $\tau = 0.5$ . This figure can be compared with Fig. 8. Here again, regular motion is observed for  $\alpha > 0.0145$  as in the case

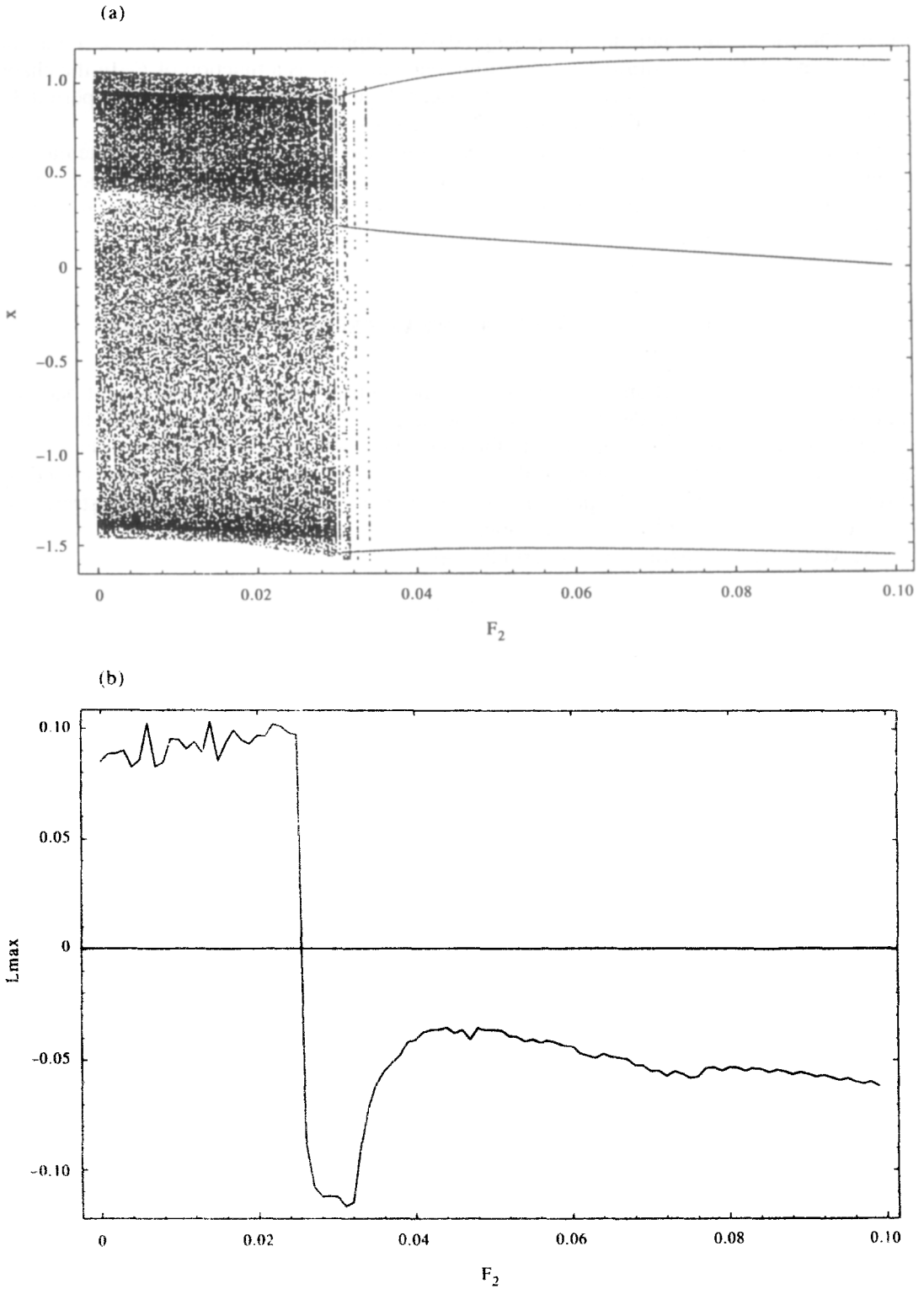


Fig. 6. (a) Bifurcation diagram of eqns (3), with  $\sigma = 1.015$ ,  $\beta = 1$ ,  $F_1 = 0.15$ ,  $\omega_1 = 0.75$ ,  $a = -1.02$ ,  $b = -0.55$ ,  $\omega_2 = 0.75$ . (b) The maximal Lyapunov exponent spectrum in  $(\lambda_{\max} - F_2)$  plane.

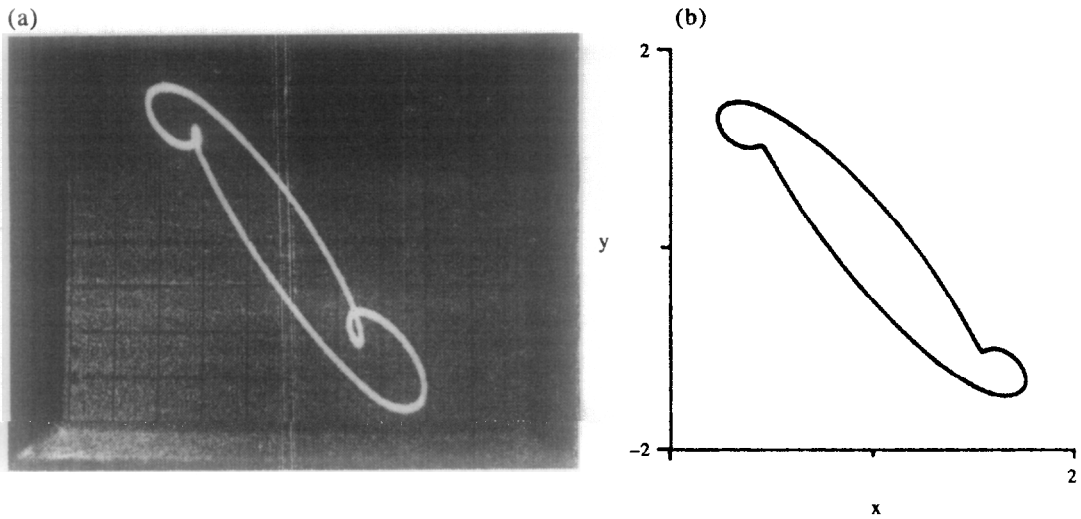


Fig. 7. Controlled period- $3T$  attractors of (a) the MLC circuit, (b) eqns (3) for  $F_2 = 0.06$ .

when  $\delta(t)$  is nonzero at  $t = n\tau T$ . Thus, small deviations in the times at which the force  $\delta(t)$  is nonzero seem to have no negative effect on the suppression of chaos. However, the system shows noisy type inverse period-doubling phenomenon.

Further, the effect of phase difference  $\phi$  between the periodic external force  $F \sin \omega t$  and  $\delta(t)$  is also studied. For various values of  $\tau$  and  $\alpha$ , the dynamics of the MLC equation is

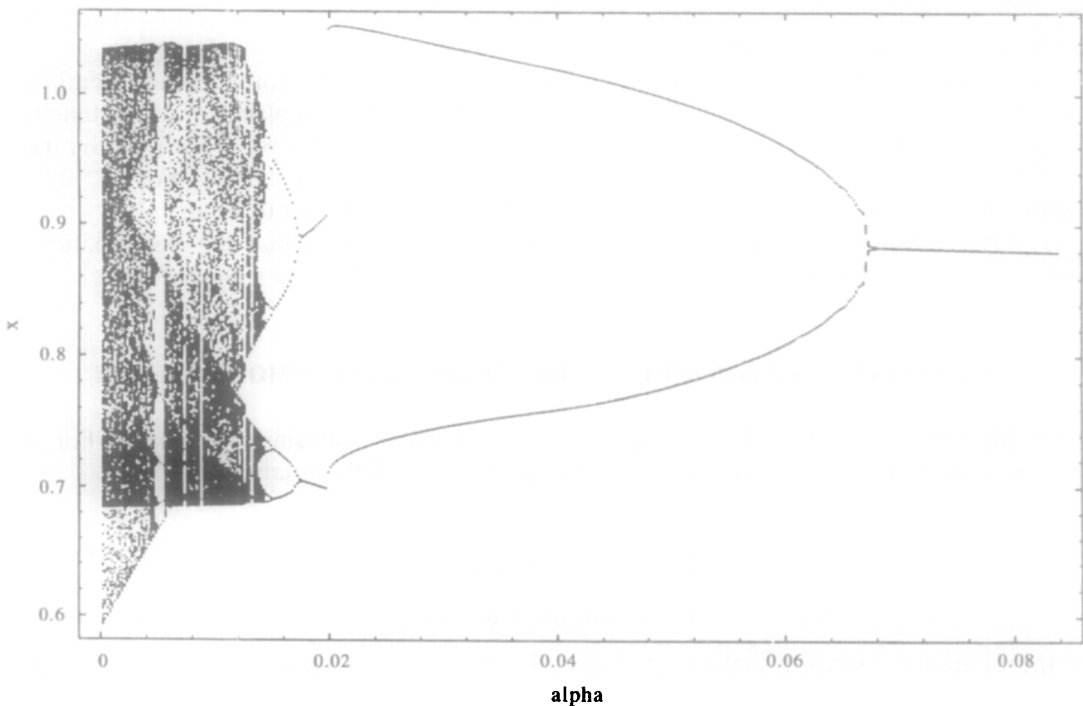


Fig. 8. Bifurcation diagram of eqns (4) as a function of  $\alpha$ , with  $\sigma = 1.015$ ,  $\beta = 1$ ,  $a = -1.02$ ,  $b = -0.55$ ,  $\omega = 0.75$ ,  $F = 0.1$ ,  $\tau = 0.5$ ,  $T = 2\pi/\omega$ .

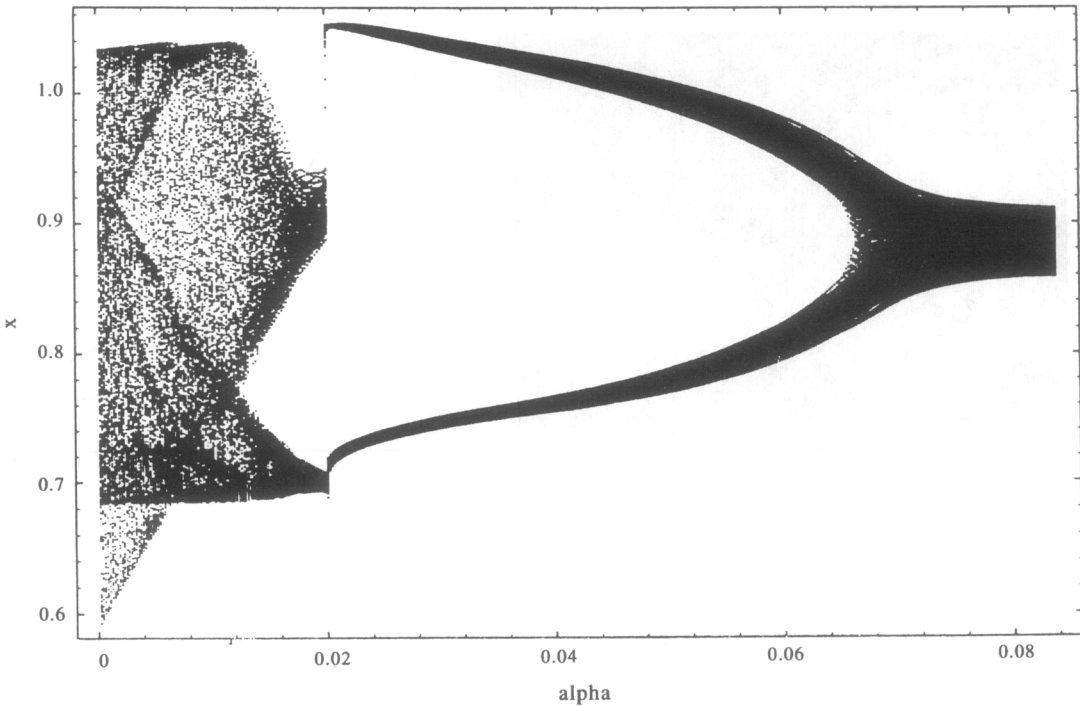


Fig. 9. Bifurcation diagram of eqns (4) for  $\tau = 0.5$ , with the  $\delta$ -force applied at one of the times  $n\tau T$ ,  $n\tau T \pm \Delta t$ , randomly for each value of  $n$ .

studied by varying  $\phi$ . Interestingly, the behaviour of the system whether it is chaotic or periodic is unaltered by the presence of  $\phi$ . The only effect observed is an infinitesimal shift in the values of the state variables in the Poincaré map.

The possibility of controlling chaos by weak periodic rectangular force of short width has also been studied. For this analysis, the delta function force is replaced by a rectangular force  $g(t)$ , where  $g(t) = \alpha$ , for  $0 \leq t \leq 0.02T$ ,  $0.48T \leq t \leq 0.52T$  and  $0.98T \leq t \leq T$ , with  $t \bmod T$ . Otherwise,  $g(t) = 0$ . Chaotic motion is found to persist for  $\alpha \leq 0.004$ . For  $\alpha > 0.004$ , suppression of chaos by inverse period-doubling bifurcation is found to occur.

A prime advantage of the addition of periodic pulse train is that the perturbation is discontinuous, that is, the system is disturbed only at specific discrete values of time.

#### 4. ENTRAINMENT CONTROL IN THE FITZHUGH–NAGUMO EQUATION

In this section, we describe the suppression of chaos by entrainment control. For the purposes of illustration, we choose the FitzHugh–Nagumo (FN) equation [15]

$$\dot{V} = W, \tag{5a}$$

$$\dot{W} = -V^3 + V/3 + R - uW, \tag{5b}$$

$$\dot{R} = -(c/u)(V + a - bR), \tag{5c}$$

as the reference system. Equations (5a)–(5c) describe the propagation of nerve pulses in a neuronal membrane with  $V$  and  $R$  being the voltage across the membrane and the recovery variable, respectively, and  $a$ ,  $b$ ,  $c$  and  $u$  are constant parameters. We fix these parameters in a chaotic region and study the suppression of chaos by entraining the FN system dynamics

to a chosen stationary point solution and to a limit cycle motion. First, we briefly discuss the basic idea of entrainment control [10, 11].

Let us consider a system of the form

$$\dot{x} = E(x), \quad (6)$$

where  $x = (x_1, x_2, \dots, x_n)^T$  and  $E(x)$  is differentiable. To entrain the dynamics of equation (6) to a desired goal orbit  $g$  which is not a particular solution of equation (6), we add the action  $F(g, \dot{g})$  to the right-hand side of equation (6) so that it becomes

$$\dot{x} = E(x) + F(g, \dot{g})S(t), \quad (7)$$

where  $S(t)$  is a switching function. For example,  $S(t) = 0$  if  $t < t_0$  and  $S(t)$  can be 1 (switched on) or 0 (switched off) if  $t \geq t_0$ . The time  $t_0$  is when  $S(t)$  is first turned on ( $S(t_0) = 1$ ). The goal orbit must be confined to convergent regions  $C_k$  of phase space of equation (6), that is,

$$g(t) \in C_k = \{x \mid |\lambda(x)\delta_{ij} - \partial E_i / \partial x_j| = 0, \text{Re } \lambda < 0, \text{ for all } \lambda; i, j = 1, \dots, n\}. \quad (8)$$

The function  $g(t)$  is a 'goal dynamics' towards which  $x(t)$  would tend if the switch remains on for all time. That is, if  $S(t) = 1$ , for all  $t > t_0$ , then the goal is to entrain the system's dynamics to  $g(t)$ , as defined by

$$\lim_{t \rightarrow \infty} |x(t) - g(t)| = 0, \quad (9)$$

for all  $x(0) \in C_k$ . If  $g(t)$  or  $x(t)$  is not in  $C_k$ , any control equation (7) will have an undesired effect. For  $x(t) = g(t)$  to be a solution of equation (7), the function  $F(g, \dot{g})$  is the Hubler action [7, 10, 11], and  $F(g, \dot{g})$  must be of the form

$$F(g, \dot{g}) = \dot{g} - E(g). \quad (10)$$

The convergent regions can be determined analytically using the Routh–Hurwitz theorem, without explicitly determining the roots  $\lambda(x)$  of the characteristic determinant.

In the FN equation, i.e. equations (5a)–(5c), chaotic motion is observed [15] for  $a = 0.6$ ,  $b = 0.5$ ,  $c = 0.1$  and  $u = 0.72$ . Suppose that we wish to suppress the chaotic dynamics by entraining the system to a chosen goal orbit  $g(t)$ . Now the system with the entrainment control is written as

$$\dot{V} = W + (\dot{g}_V - g_W)S(t), \quad (11a)$$

$$\dot{W} = -V + (V^3/3) + R - uW + (\dot{g}_W + g_V - g^3_V/3 - g_R + ug_W)S(t), \quad (11b)$$

$$\dot{R} = -(c/u)(V + a - bR) + (\dot{g}_R + (c/u)(g_V + a - bg_R))S(t). \quad (11c)$$

The convergent regions of the phase space of the uncontrolled FN system are the connected region  $C_k$  in which all the roots of the polynomial equation (see equation (8))

$$\lambda^3 + a_1\lambda^2 + a_2\lambda + a_3 = 0,$$

where  $a_1 = (u^2 - bc)/u$ ,  $a_2 = 1 - V^2 - bc$ ,  $a_3 = (c + bc(V^2 - 1))/u$ , have negative real parts. The necessary and sufficient conditions for all  $\text{Re } \lambda$  to be less than zero are given by the Routh–Hurwitz conditions  $a_1 > 0$ ,  $a_1a_2 - a_3 > 0$ ,  $a_3 > 0$ . These are given by

$$u^2 > bc, \quad V^2 < u^2 + b^2c^2 - bcu^2 - c, \quad V^2 > (b - 1)/b. \quad (12)$$

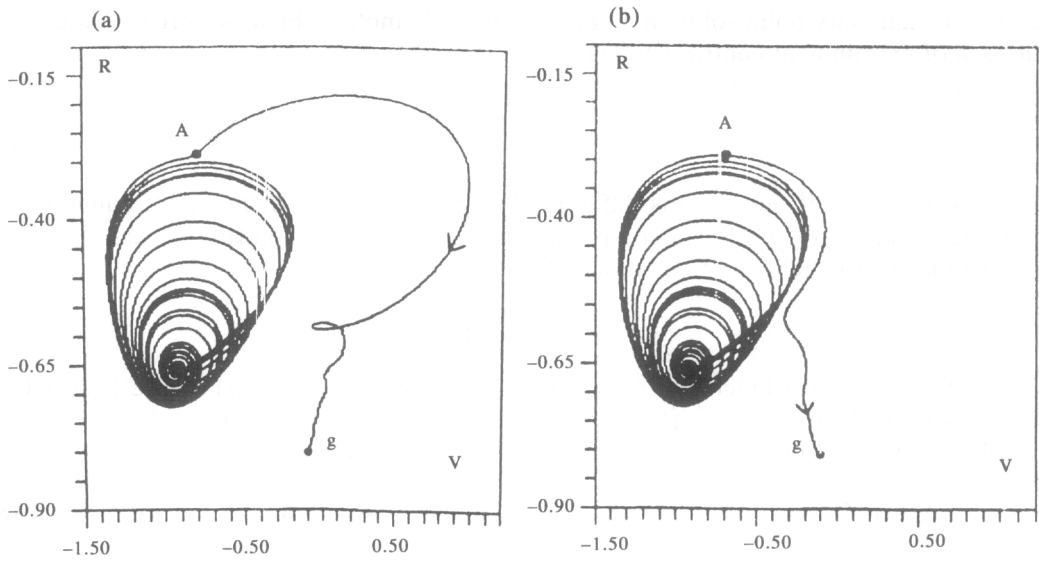


Fig. 10. Entrainment of the FN system dynamics to the goal orbit given by eqn (13), with (a) the switching function (14) and (b) the switching function (15).

These conditions involve only  $V$  and are independent of  $W$  and  $R$ . For the parametric values fixed above, the conditions are satisfied for  $V \in (-0.84, 10.84)$  and  $W$  and  $R$  arbitrary.

First, we choose the goal dynamics as a stationary solution given by

$$(g_V, g_W, g_R) = (-0.1, 0, -0.8), \tag{13}$$

which lies in the convergent region. The switching function is chosen as

$$S(t) = \begin{cases} 0, & t < 0, \\ 1, & t \geq 0. \end{cases} \tag{14}$$

The controlled system is integrated with a step size of  $\Delta t = 0.05$ . Initial conditions used are  $(V(0), W(0), R(0)) = (-0.75, 0, -0.5)$ . Figure 10(a) shows the response of the system. The system is allowed to evolve chaotically for some time and then control is initiated when the trajectory reached the point  $A$ , lying in the convergent region, marked in Fig. 10(a). Under the action of the control, chaotic motion is suppressed and the long time evolution is entrained to the goal dynamics  $g$ . The desired control  $g$  is not achieved when it is chosen outside the convergent region. The response of the system to the switching function of the form

$$S(t) = 1 - e^{-\lambda t} \tag{15}$$

where  $\lambda > 0$ , is also studied. Figure 10(b) illustrates the smooth entrainment to the goal orbit  $g$  for  $\lambda = 0.1$ . The desired entrainment is observed for  $\lambda > 0$ .

Conversion of the system dynamics to a periodic motion has also been studied. We choose the desired goal orbit as

$$g_V = -0.6 + 0.1 \cos t, \tag{16a}$$

$$g_W = \dot{g}_V, \tag{16b}$$

$$g_R = -0.5 + 0.1 \sin t. \tag{16c}$$

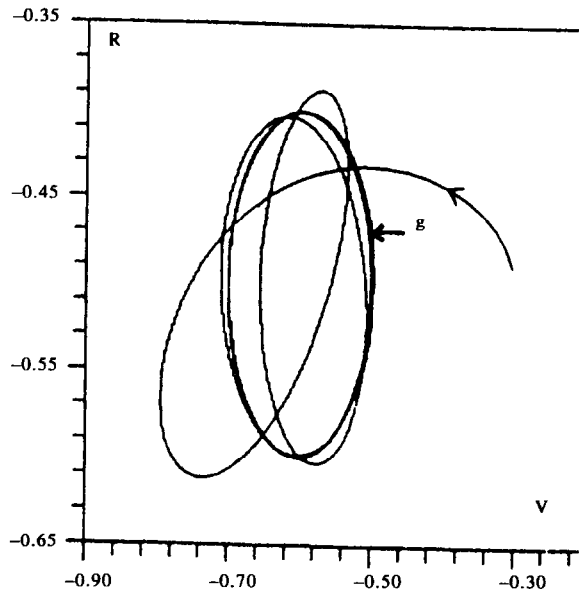


Fig. 11. Response of the FN system to the periodic goal orbit (16).

Figure 11 shows the entrainment to this periodic orbit where  $S(t)$  is given by equation (14).

From the above study, it is clear that chaotic motion in a system can be suppressed by entraining the system to a desired goal orbit. An interesting observation is that the control is nonfeedback. From equation (6), we note that if a term in  $E(x)$  is an explicit function of time only then this term will not appear in the controlled equation (7). Thus, the method is more suitable to autonomous systems than nonautonomous systems.

A prime advantage of open-loop entrainment control is that control is always guaranteed if the desired goal and the initial conditions are in the convergent region of the phase space of the given system. A prime disadvantage is that to implement entrainment control the evolution equation must be known.

## 5. SUMMARY AND CONCLUSIONS

In this paper, we have briefly discussed the controlling of chaos in the MLC circuit by different nonfeedback methods and suppression of chaos by entrainment control in the FN equation. The various nonfeedback methods considered here show different regions of applicability and efficacy. A prime advantage of the addition of periodic perturbations is that they can be easily implemented in many experimental systems as shown for the MLC circuit. Since the addition of a second periodic force and weak periodic pulses have two parameters, namely, amplitude and period, one has to identify regular and chaotic regions in the two-parameters space to choose suitable values of amplitude and period of the perturbation to realize periodic motion. In contrast to this, in the constant bias method we have a single parameter which greatly reduces the analysis of controlled system. Interestingly, a chaotic system can be entrained to any arbitrary goal dynamics lying in the convergent region of the phase space of a system and the desired goal may be a fixed point or periodic orbit or even a quasiperiodic orbit.

*Acknowledgement*—The work of K. M. and M. L. forms part of a Department of Science and Technology, Government of India sponsored research project.

## REFERENCES

1. Huberman, B. A. and Lumer, L., Dynamics of adaptive systems. *IEEE Trans. Circuits Systems*, 1990, **37**, 547–549.
2. Sinha, S., Ramaswamy, R. and Rao, Subba J., Adaptive control in nonlinear dynamics. *Phys. D*, 1990, **43**, 118–128.
3. Ott, E., Grebogi, C. and Yorke, J., Controlling chaos. *Phys. Rev. Lett.*, 1990, **64**, 1196–1199.
4. Singer, J., Wang, Y. Z. and Bau, H. H., Controlling a chaotic system. *Phys. Rev. Lett.*, 1991, **66**, 1123–1125.
5. Pyragas, K., Continuous control of chaos by self-controlling feedback. *Phys. Lett. A*, 1992, **170**, 421–428.
6. Chen, G. and Dong, X., On feedback control of chaotic dynamic systems. *Int. J. Bifurcation and Chaos*, 1992, **2**, 407–411.
7. Jackson, E. A., OPCL migration controls between five attractors of the Chua system. *Int. J. Bifurcation and Chaos*, 1995, **5**, 1255–1260.
8. Lima, R. and Pettini, M., Suppression of chaos by resonant parametric perturbations. *Phys. Rev. A*, 1990, **41**, 726–733.
9. Braiman, Y. and Goldhirsch, I., Taming chaotic dynamics with weak periodic perturbations. *Phys. Rev. Lett.*, 1991, **66**, 2545–2548.
10. Hübler, A. and Lüscher, E., Resonant stimulation and control of nonlinear oscillators. *Naturwissenschaften*, 1989, **76**, 67–69.
11. Jackson, E. A., Controls of dynamic flows with attractors. *Phys. Rev. A*, 1991, **44**, 4839–4853.
12. Rajasekar, S. and Lakshmanan, M., Algorithms for controlling chaotic motion: application for the BVP oscillator. *Phys. D*, 1993, **67**, 282–300.
13. Murali, K. and Lakshmanan, M., Controlling of chaos in driven Chua's circuit. *J. Circuits Systems Comput.*, 1993, **3**, 125–137.
14. Rajasekar, S., Controlling of chaotic motion by chaos and noise signals in a logistic map and a Bonhoeffer–van der Pol oscillator. *Phys. Rev. E*, 1995, **51**, 775–778.
15. Rajasekar, S. and Lakshmanan, M., Bifurcation, chaos and suppression of chaos in FitzHugh–Nagumo nerve conduction model equation. *J. Theor. Biol.*, 1994, **166**, 275–288.
16. Murali, K., Lakshmanan, M. and Chua, L. O., Controlling and synchronization of chaos in the simplest dissipative non-autonomous circuit. *Int. J. Bifurcation and Chaos*, 1995, **5**, 563–571.
17. Lakshmanan, M. and Murali, K., *Chaos in Nonlinear Oscillators: Controlling and Synchronization*. World Scientific, Singapore, 1996.
18. Lakshmanan, M. and Rajasekar, S., Directing chaotic systems to regular motion. In *Proceedings of National Academy of Sciences (India)*, 1996.